JOURNAL OF MATERIALS SCIENCE 25 (1990) 1833–1841

Rheology of composite ceramic injection moulding suspensions

S. J. STEDMAN, J. R. G. EVANS
Department of Materials Technology, Brunel University, Uxbridge, Middlesex UB8 3PH, UK
J. WOODTHORPE
T & N Technology Ltd, Cawston House, Cawston, Rugby CV22 7SA, UK

Ceramic injection moulding compositions incorporating sinterable silicon nitride powder and silicon carbide whiskers were prepared by twin screw extrusion using a polypropylene-based organic vehicle. Their viscosities in the shear rate range 100 to 1400 sec^{-1} were measured by capillary rheometry. The relative viscosity (η_r)–ceramic volume loading (V) curve fitted the Chong equation

$$\eta_r = \left(1 + \frac{0.75\, V/V_{max}}{1 - V/V_{max}}\right)^2$$

where V_{max} is the volume loading of ceramic at which viscosity approaches infinity. This equation fitted the data for compositions containing ceramic powder as well as particle–whisker suspensions and could thus be used to map relative viscosity as a function of filler loading for all compositions with 0 to 30% SiC based on the ceramic.

1. Introduction

The strength and reliability of technical ceramics may be improved by two approaches. In the first place there is considerable interest in the minimization of critical defect size by attention to particle size, shape and packing [1]. In the second place, the fracture toughness may be increased by the incorporation of crack-arresting second phases [2], by transformation toughening [3] and latterly by the incorporation of whiskers [4, 5]. The reinforcing effect of whiskers or fibres may be effective if the whisker/matrix modulus ratio is greater than 2 [6]. Although this is not the case for silicon carbide whiskers ($E \sim 480$ GPa) [7] embedded in a silicon nitride matrix ($E \sim 352$ GPa) [8], other toughening mechanisms may be active. In particular, the effect of crack deflection at the whisker–matrix interface [9] and the absorption of energy by whisker pull-out [10] may contribute to increased work of fracture. Furthermore, whiskers may inhibit grain-boundary sliding under creep conditions and may also have the advantage of reducing grain growth during sintering.

The presence of whiskers in a particle assembly unfortunately presents considerable difficulties for processing. The approach of particle centres during sintering is hindered and therefore full density is not achieved without the application of external pressure. The arrangement of particles into a useful shape is also made difficult by the presence of whiskers and much early work relied on slurry processing [11]. The injection moulding of composite ceramics is possible [12] and provides a rapid assembly process suitable for mass production [13, 14].

In the present work, the effect of whisker additions on the rheology of ceramic injection moulding blends is investigated. The rheological requirements of ceramic injection moulding blends in terms of fluidity, flow behaviour index and temperature dependence of fluidity have been established [15]. Fluidity is strongly influenced by ceramic powder loading. Although the relationship between relative viscosity of a suspension and powder volume loading has been investigated thoroughly at low volume loadings [16], at high volume loadings ($V > 0.5$) there are only a few semi-empirical equations which fit experimental data. The behaviour of particle–rod assemblies is less well understood. Milewski [17] has studied the packing efficiency of particle–rod assemblies as a function of aspect ratio, particle to rod radius ratio and volume fraction of rods. Because most relative viscosity–volume loading relationships contain V_{max}, the maximum packing efficiency, as a constant [18], this work may be useful in predicting viscosity.

2. Experimental details

2.1. Materials

Silicon carbide whiskers (Grade SCW 1) were obtained from Tateho Chemical Industries, Ako-Shi, Japan. The silicon nitride powder was grade Nu-10 from Showa Denko Co. Ltd, Tokyo, Japan and was milled with 5.0 wt % Y_2O_3 concentrate (yttrium concentrate, Rare Earth Products Ltd, Widnes, UK) and 5.5 wt %

0022–2461/90 $03.00 + .12

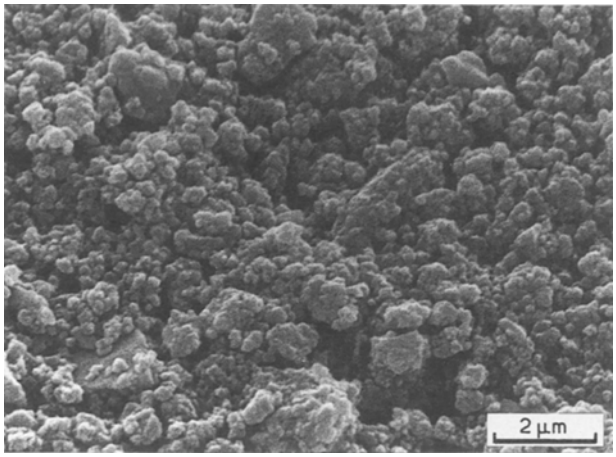

Figure 1 Scanning electron micrograph of Showa Denko silicon nitride powder after milling with sintering ends.

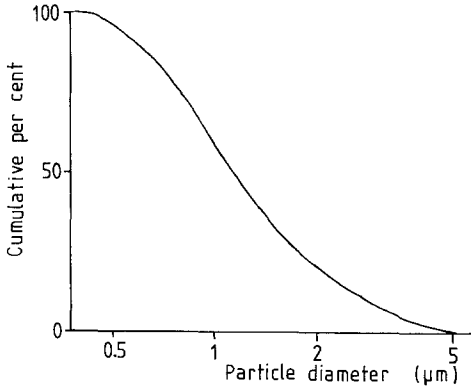

Figure 2 Particle size distribution for silicon nitride powder after milling with sintering ends.

Al_2O_3 as sintering aids at the laboratories of T & N Technology Ltd.

Scanning electron micrographs of the silicon nitride powder and the silicon carbide whiskers are shown in Figs 1 and 3, respectively. The polypropylene (pp) was GY545M from ICI plc and the microcrystalline wax was Okerin 1865Q from Astor Chemicals Ltd, Middlesex, UK. Stearic acid was purchased from BDH Chemicals Ltd, West Drayton, UK. The compositions prepared are given in Table I which also includes the exact volume percentage of ceramic calculated from the mean of four ashing trials after mixing.

The silicon carbide whiskers and silicon nitride powder were precoated with stearic acid in a solution of carbon tetrachloride. The solvent was then evaporated and finally the whisker/powder mixture was dried under vacuum. The ceramic mixture and remaining organic constituents were preblended in a low-speed rotary mixer (Moritz Chemical Engineering Co, UK). This preblend was then transferred to a Betol TS40 twin screw extruder with barrel temperatures (feed to exit) of 210, 215, 225, 215° C. The extrudate was cooled in a water bath and granulated after drying.

Compositions containing silicon nitride only were preblended in a Henschel high-speed non-refluxing mixer before the twin screw extrusion stage.

2.2. Rheological measurements

The flow properties were measured using a Davenport capillary rheometer at 225° C. Initially, dies of diameter 1.5 mm and lengths 10, 20 and 35 mm were used to obtain an end correction. The latter proved to be very small and in the remaining work the 35 mm die was used and the end correction was neglected. After charging the barrel and waiting 10 min for temperature equilibration, the pressure drop over the die was

TABLE I

Composition	0	SN50	SN57.5	SN60	SN63	SN67	C1	C2	C3	C4	C5	C6
Intended volume loading (%)	–	50.0	57.5	60.0	63.0	67.0	50.0	53.0	56.0	50.0	50.0	50.0
Measured volume loading (%)	–	50.2	57.4	60.1	63.0	66.9	50.1	53.2	55.6	50.8	48.8	50.4
SiC whisker fraction of ceramic	–	0	0	0	0	0	0.2	0.2	0.2	0.23	0.27	0.30
SiC (wt %)	–	–	–	–	–	–	15.3	15.7	16.0	17.6	20.7	23.0
Si_3N_4 (wt %)	–	78.5	83.2	84.5	86.1	88.0	63.1	64.7	66.2	63.7	60.4	55.3
PP (wt %)	66.7	14.3	11.2	10.3	9.2	8.0	14.4	13.3	11.9	14.4	14.5	14.5
Wax (wt %)	22.2	4.8	3.7	3.5	3.1	2.7	4.8	4.4	4.0	4.8	4.8	4.8
Stearic acid (wt %)	11.1	2.4	1.9	1.7	1.6	1.3	2.4	2.2	2.0	2.4	2.4	2.4
Measured relative viscosity	1.0	6.5	11.7	16.4	21.2	–	14.8	27.3	35.2	19.4	18.3	30.9
Power law index, *n*	–	0.7	0.8	0.8	0.8	–	0.5	0.4	0.5	0.5	0.5	0.4

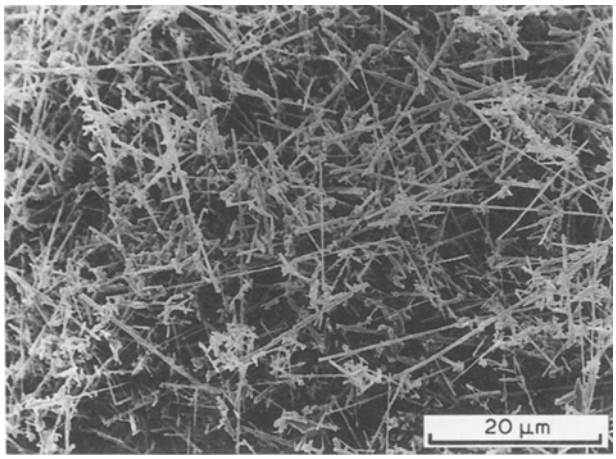

Figure 3 Scanning electron micrograph of the as-received Tateho silicon carbide whiskers.

measured using a 34.45 or 68.9 N mm^{-2} full-scale transducer as appropriate, in the shear rate range 100 to 1400 sec^{-1}. This includes the range of shear rates encountered in the injection-moulding process. The viscosity data were corrected for non-Newtonian flow using the Rabinowitsch correction [19].

3. Results and discussion

3.1. Preparation of suspension

The silicon nitride (Fig. 1) was a submicrometre powder which tended to show agglomerates in the 2 to 5 μm region. The particle size distribution obtained by a Coulter Counter method (Fig. 2) probably reflects the state of agglomeration. The silicon carbide whiskers in the form in which they were received are shown in Fig. 3. The whiskers have diameters in the range 0.3 to 1.5 μm and after processing by extrusion they have a mean length of 12 μm. The length distribution was measured on dispersed samples using an optical microscopy imaging method to be described in full elsewhere [20] and not by cursory inspection of scanning electron micrographs. It is noteworthy that the whiskers appear in the undispersed form to have greater average length than that measured by imaging of a dispersed sample. This illustrates the difficulty in assessing length and hence aspect ratio from an undispersed mat of whiskers. On the basis of these measurements, aspect ratios before processing fall in the 8 to 40 range but because the whisker length varies from 3 to 30 μm the actual range of aspect ratio is much greater.

The procedure for precoating the whiskers with stearic acid considerably assisted the preparation of the suspensions [20] and this can be attributed to the lubricant action of carboxylic acid layers [21].

3.2. Viscosity of Si_3N_4 suspensions

The viscosity–shear rate plot for compositions containing only silicon nitride at a range of volume loadings (Fig. 4) shows that all the suspensions have the pseudo-plastic behaviour of a power law fluid and fit the relationship

$$\eta = k\dot{\gamma}^{n-1} \quad (1)$$

where η is the viscosity, $\dot{\gamma}$ is the shear rate, k is a constant and n is the flow behaviour index. The flow behaviour indices were in the range 0.7 to 0.8 indicating that even at high shear rates signs of dilatancy were absent.

It has been suggested that for ceramic injection moulding the maximum viscosity at the lower end of the shear rate range encountered in injection moulding (100 sec^{-1}) should be in the region 1000 to 1400 Pa sec depending on the capability of the machine and the cavity design. In the present work, viscosities which had been corrected by the Rabinowitsch correction

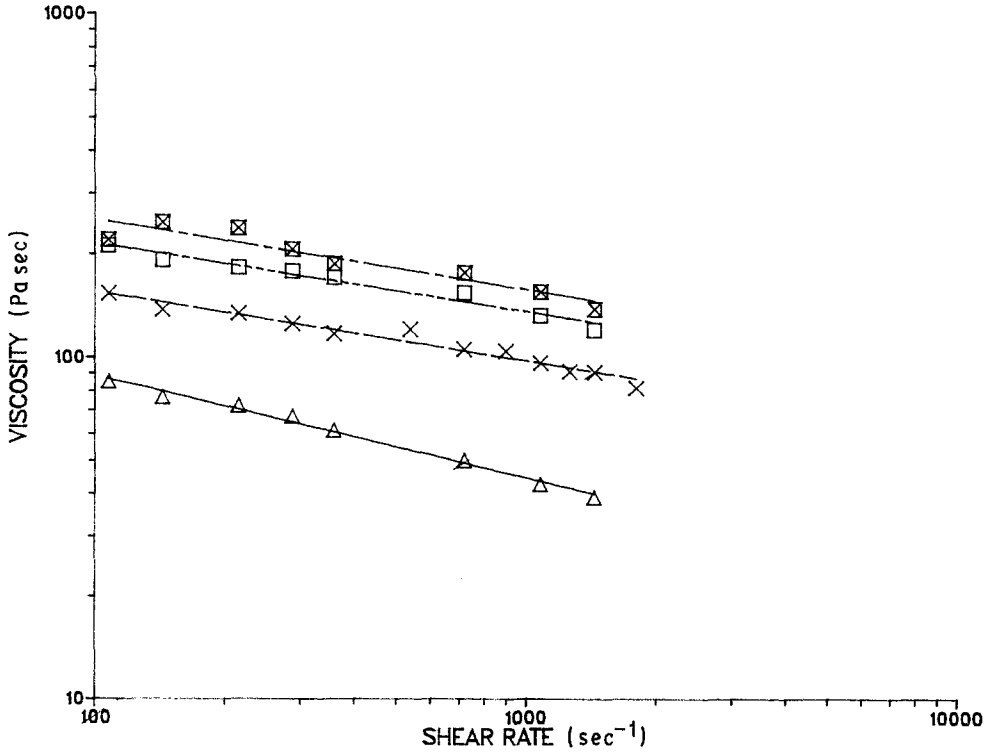

Figure 4 Viscosity–shear rate plots for silicon nitride suspensions with (Δ) 50 vol %, (×) 57.5 vol %, (□) 60 vol % and (⊠) 63 vol % powder.

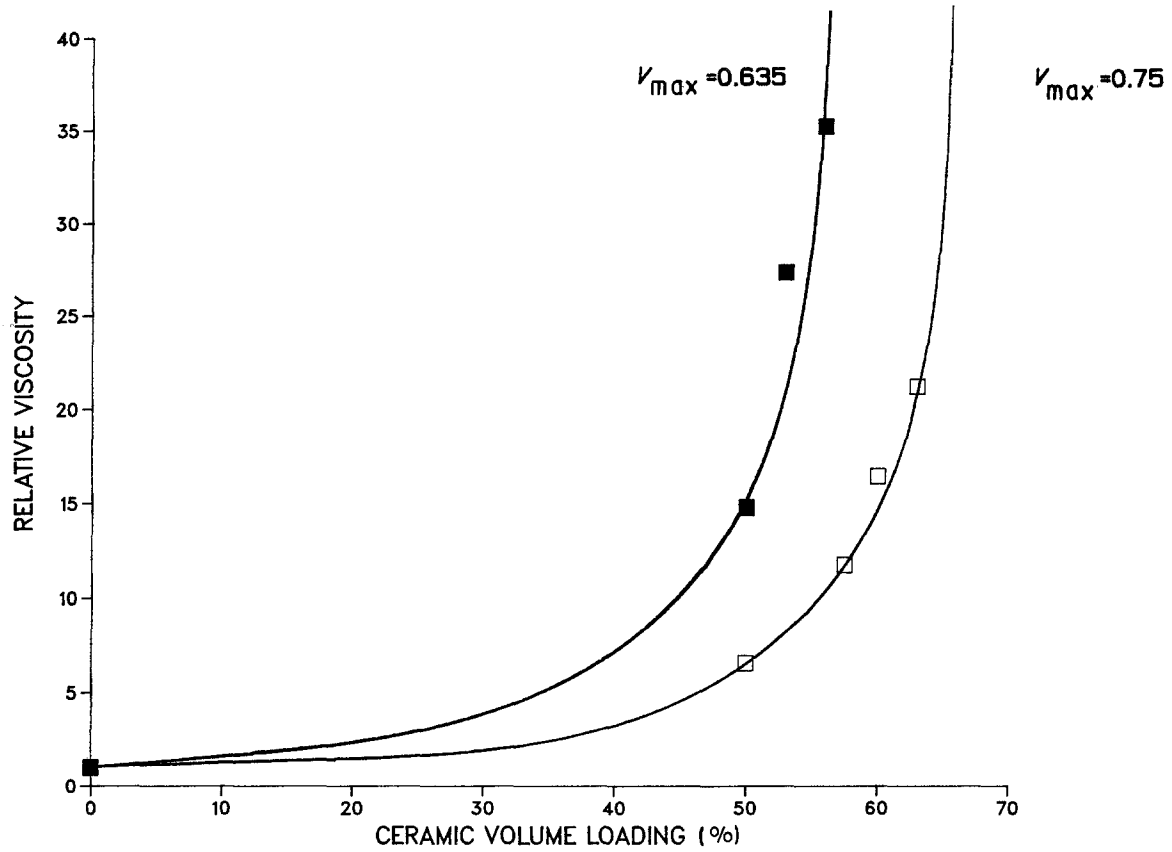

Figure 5 Relative viscosity–volume loading curve for (□) the silicon nitride powder from Fig. 4 and ■ the composite suspension from Fig. 7. Shear rate = 143 sec^{-1}.

were recorded at 143 sec^{-1} and compared. The viscosity of the unfilled polymer blend η_0 (composition 0) was measured as 16 Pa sec at 143 sec^{-1}. The relative viscosities (η_r) of the filled compositions were then calculated from

$$\eta_r = \eta/\eta_0 \quad (2)$$

and were plotted as a function of volume loading (Fig. 5). This curve shows that at high volume loadings of ceramic powder, viscosity approaches infinity. A characteristic of this curve is V_{max}, the volume loading at which the viscosity becomes infinite as particles make contact or are inhibited from rotating in shear flow. In principle, V_{max} is related to the maximum packing efficiency of the powder and is dependent on powder characteristics such as particle size distribution, particle shape and specific surface area.

3.3. Prediction of the viscosity of suspensions

A number of expressions have been derived to relate relative viscosity to volume loading for concentrated suspensions. A characteristic of many such semi-empirical equations is that they include a function of $(V_{max} - V)$ as denominator. Thus viscosity is related to the extra volume fraction of organic vehicle $(V_{max} - V)$ over and above that needed to fill the interstices between contacting particles $(1 - V_{max})$.

Eilers [22] suggested that

$$\eta_r = \left(1 + \frac{1.25V}{1 - V/V_{max}}\right)^2 \quad (3)$$

Mooney [23] presented the relationship

$$\eta_r = \exp\left(\frac{2.5V}{1 - kV}\right) \quad (4)$$

where k was taken as $1/V_{max}$ for monosized spheres. Chong *et al.* [24] modified Eilers' equation to produce an equation which fits experimental data close to V_{max}

$$\eta_r = \left(1 + \frac{0.75V/V_{max}}{1 - V/V_{max}}\right)^2 \quad (5)$$

Figure 5 shows the experimental data for silicon nitride (compositions SN50-SN63) and the best fit of Equation 5 obtained by an iterative method. Mooney's equation gives $V_{max} = 1.2$ and is a poor fit to data points above $V = 0.5$, clearly this V_{max} is not valid. Eilers gives $V_{max} = 0.81$ and presents a better fit.

Chong's equation gives the best fit and $V_{max} = 0.75$. For monosized particles, random close packing would give $V_{max} = 0.635$ [25] and the maximum possible ordered packing would be 0.74. The higher value of V_{max} observed for the silicon nitride powder is expected from the wider particle size distribution shown in Fig. 1 [26].

Theoretical methods of predicting the porosity [27–29] or the maximum solids loading [30, 31] of polydisperse systems from powder characteristics have been developed. However, application of these theories to highly concentrated suspensions is only valid for well-dispersed particles [32] and wide discrepancies between experimental and calculated theoretical maximum solids loadings have been found [33]. The analytical methods ignore the effect of particle

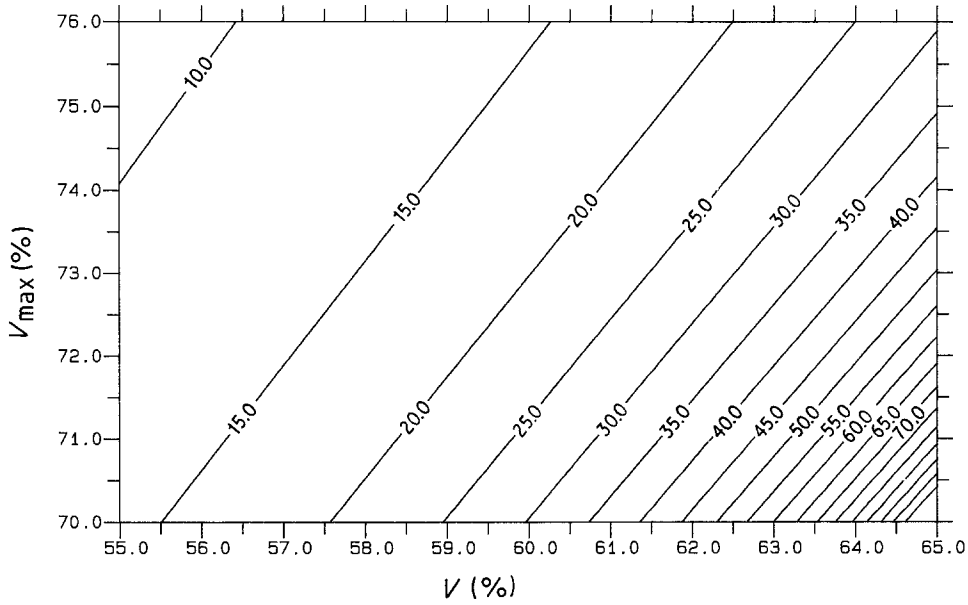

Figure 6 Contour map for Chong's equation allowing prediction of relative viscosity from a single measurement. Contours are labelled with relative viscosity values.

surface chemistry and particle shape on the packing configuration.

The equation of Chong *et al.* [24] provides a route to the direct prediction of viscosity if V_{max} could be predicted from powder properties. However, it should be noted that the steep gradient of the relative viscosity curves in the region which is of interest for injection moulding, demands an accuracy in predicted V_{max} of about 1 vol % if it is to serve a useful purpose. Probably the most serious threat to this accuracy is the fact that particle size distribution curves such as that in Fig. 2 do not always present data for deagglomerated powder. Thus, if intensive mixing devices used in preparing ceramic injection moulding formulations are more effective in dispersion than the method used for deagglomeration in particle size measurement then the particle size distribution so obtained would not be suitable for calculation of V_{max}.

The excellent fit of Chong's equation to ceramic injection moulding suspensions in the present work and also in related work [18, 33] suggests that provided the viscosity of the organic binder is known under some chosen conditions, a single measurement of viscosity of a ceramic moulding suspension yields the full viscosity curve. The measured composition should fall in the high volume loading regime. This avoids the need to prepare a series of blends for each new powder or powder batch encountered. The optimum ceramic powder loading can be selected from a single experiment without a knowledge of particle characteristics.

Fig. 6 presents a contour map for the equation of Chong *et al.* for a range of volume fractions relevant to ceramic injection moulding (V = 0.55 to 0.65 and for a range of V_{max} from 0.70 to 0.76). By making use of this map, the relative viscosity curve for a given powder can be obtained from one measurement of viscosity of a crowded suspension and from this curve the volume fraction needed to give a suitable viscosity for injection moulding, typically 1000 to 1400 Pa sec [15] can be found.

3.4. Viscosity of composite suspensions

The problem of selecting a suitable volume fraction of ceramic is further complicated by whisker additions because a formidable array of possible compositions present themselves and a considerable supply of silicon carbide whiskers would be required for exhaustive exploration.

Compositions C1 to C3 were prepared incorporating a ceramic content based on 20 vol % SiC whiskers 80 vol % Si_3N_4 powder at various volume loadings in the same organic vehicle. Fig. 7 shows the log viscosity–log shear rate plots for these compositions. The lower overall volume loadings of ceramic were necessitated by the inferior packing of the powder–whisker blend as expected. The suspension also showed pseudoplastic behaviour with the flow behaviour index, n, in the region 0.4 to 0.5.

These suspensions are clearly more pseudoplastic than the suspensions containing silicon nitride only, despite the fact that they are based on the same organic vehicle. There are two possible explanations for this observation. It is possible that whisker length degradation occurred at high shear stresses resulting in a genuinely lower viscosity suspension. It is also possible that whisker orientation occurred at higher shear rates under converging flow and this reduced the viscosity [34, 35]. Once again, viscosity readings at the low shear rate end (143 sec^{-1}) were used to construct a relative viscosity–volume loading curve, which is shown in Fig. 5. Surprisingly, Chong's equation also fits these data well giving a much lower V_{max} of 63.5 vol %. This reduction from 75 vol % is a consequence of replacing some of the silicon nitride to give a 20 vol % silicon carbide whisker blend. Thus in the region of volume loadings of interest in ceramic injection moulding, where the two curves are almost parallel, the 20% whisker substitution means that the overall ceramic volume loading must be reduced by about 11 vol % to yield the same viscosity as the silicon nitride suspension.

Previous validations of Chong's equation have used

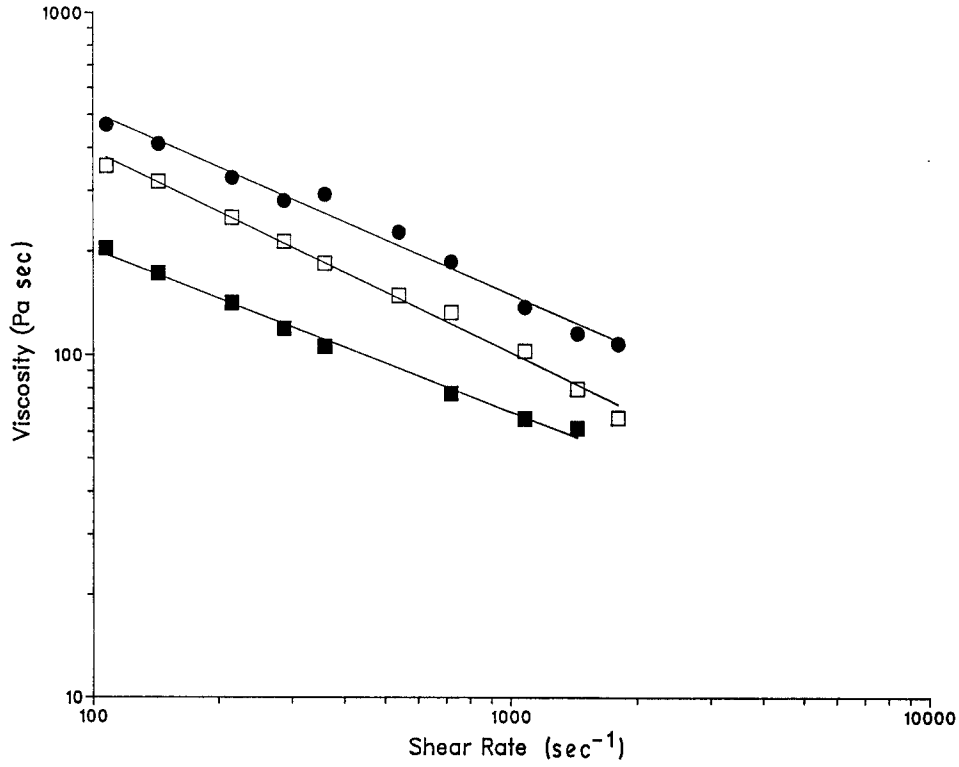

Figure 7 Viscosity–shear rate plots for 20 vol % SiC whiskers: 80 vol % Si_3N_4 powder at (■) 50 vol %, (□) 53 vol % and (●) 56 vol %.

spherical or equaxed particles and the observation that data for a particle–rod suspension also agrees with the equation is both novel and extends the versatility of the relationship.

Other relative viscosity–volume loading relationships which have been specified for eliptical particles appear to be less satisfactory because they cannot be directly applied to a composite system. Brodnyan [36] extended Mooneys equation to consider ellipsoidal particles

$$\eta_r = \exp\left(\frac{2.5V + 0.399\,(p^{-1})}{1 - kv}\,1.48V\right) \quad (6)$$

where p is the axial ratio. Similarly Kitano *et al.* [37] has developed an equation for accicular particles.

$$\eta_r = \left(1 - \frac{V}{0.54 - 0.0125p}\right)^2 \quad (7)$$

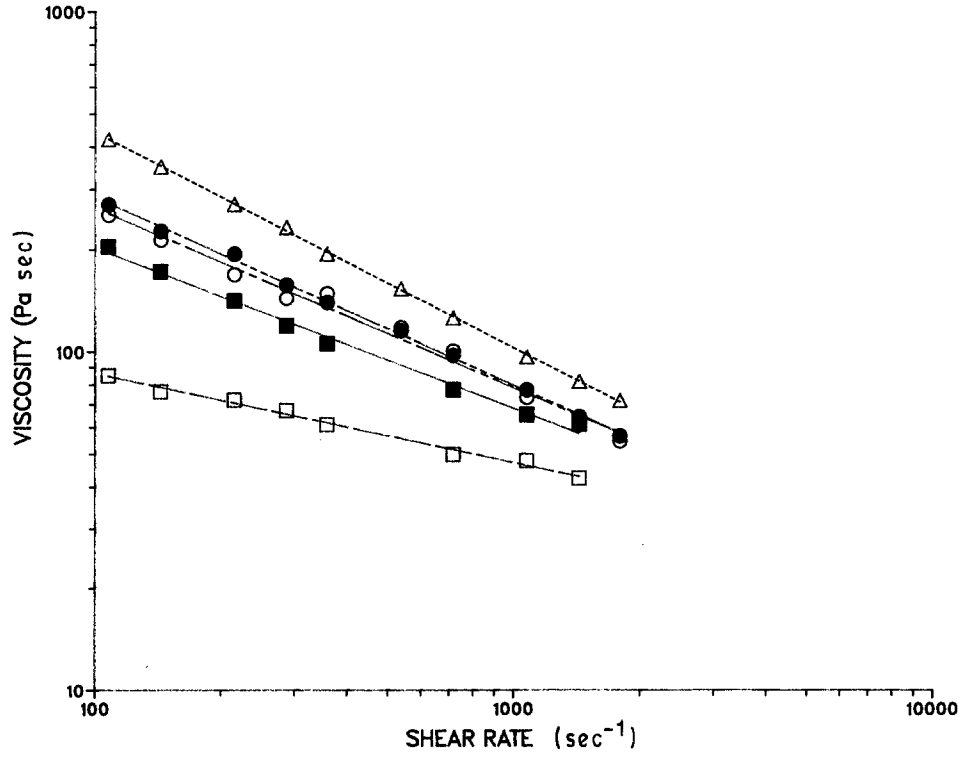

Figure 8 Viscosity–shear rate plots for 50 vol % ceramic suspension with (□) 0 vol %, (□) 20 vol % SiC, (●) 23 vol % SiC, (○) 27 vol % SiC and (△) 30 vol % SiC whisker substitutions based on the Si_3N_4 content.

TABLE II

Composition	SN50	C1	C4	C5	C6
SiC whisker fraction of ceramic	0	0.2	0.23	0.27	0.30
Measured volume (%)	50.2	50.1	50.8	48.8	50.4
Measured relative viscosity	6.5	14.8	19.4	18.3	30.9
V_{max}	0.750	0.635	0.620	0.600	0.584
Calculated relative viscosity at 50 vol %	6.4	14.3	17.0	22.6	29.9

3.5. Effect of varying whisker content

With the overall ceramic content held constant at 50 vol %, compositions SN50, C1, C4, C5 and C6 were prepared with the whisker content varying from 0 to 30 vol % ceramic. This allows the effect of increasing SiC whisker content on viscosity to be studied. The viscosity–shear rate plots are shown in Fig. 8 and there is now clear evidence of an effect of whisker content on flow behaviour index. This may result from whisker length degradation during flow in the capillary at high shear stress or whisker orientation at high shear rates [34, 35, 38]. The actual volume loading obtained from ashing results for composition C4 was lower than intended, while the volume loading for C5 was slightly higher than expected due to mixing losses. For this reason the log viscosity–log shear rate plots for these compositions are coincident. Because the relative viscosity of a filled suspension is strongly dependent upon volume loading, the comparison of suspensions containing different whisker fractions may only be undertaken if each has exactly the same volume loading. Table II shows the exact volume loadings calculated from ashing results, indicating a deviation of up to 1.2 vol % from the intended 50 vol % ceramic content. This small discrepancy results in a viscosity measurement which deviates from the value at 50 vol % ceramic content by 12%. This illustrates the necessity of controlling volume loading of ceramic with precision and emphasizes the accuracy demanded by prediction of V_{max} from particle characteristics.

In order to correct the relative viscosity values for these suspensions to correspond to 50 vol % ceramic content, the procedure used in Section 3.3 was employed. V_{max} was calculated assuming a fit to Chong's equation and the corresponding relative viscosity at 50 vol % was thereby obtained (Table II). The corrected relative viscosity of these suspensions at 143 sec^{-1} was plotted against ceramic whisker content in Fig. 9.

The abscissa in Fig. 9 is whisker volume per cent based on the ceramic. This curve shows a monotonic increase in relative viscosity with increasing whisker content. It is fortuitous that whisker contents in the 20 to 30 vol % region based on the ceramic content are effective in producing enhanced toughness [8] because viscosity rises steeply above 30%. In Fig. 9 the relative viscosity is based on the unfilled polymer blend so that for zero whisker content $\eta_r = 6.4$, which value is also seen in Fig. 5. A slight decrease in average whisker length occurs as whisker content is increased [20]. This is inevitable in the processing method employed and means that the increase in viscosity with increasing whisker content is slightly underestimated.

3.6. Mapping the viscosity of composite blends

The increase in viscosity afforded by whisker addition for a 50 vol % ceramic suspension is described by the curve in Fig. 9 and can be fitted to a polynomial to

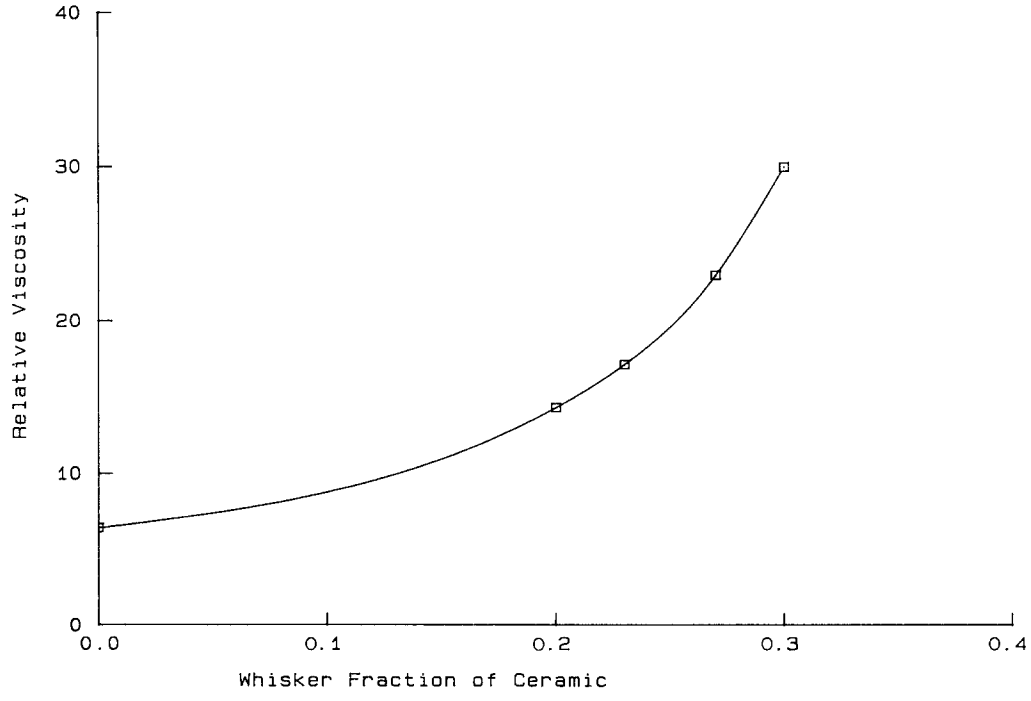

Figure 9 Relative viscosity–whisker content plot for 50 vol % composite ceramic suspension.

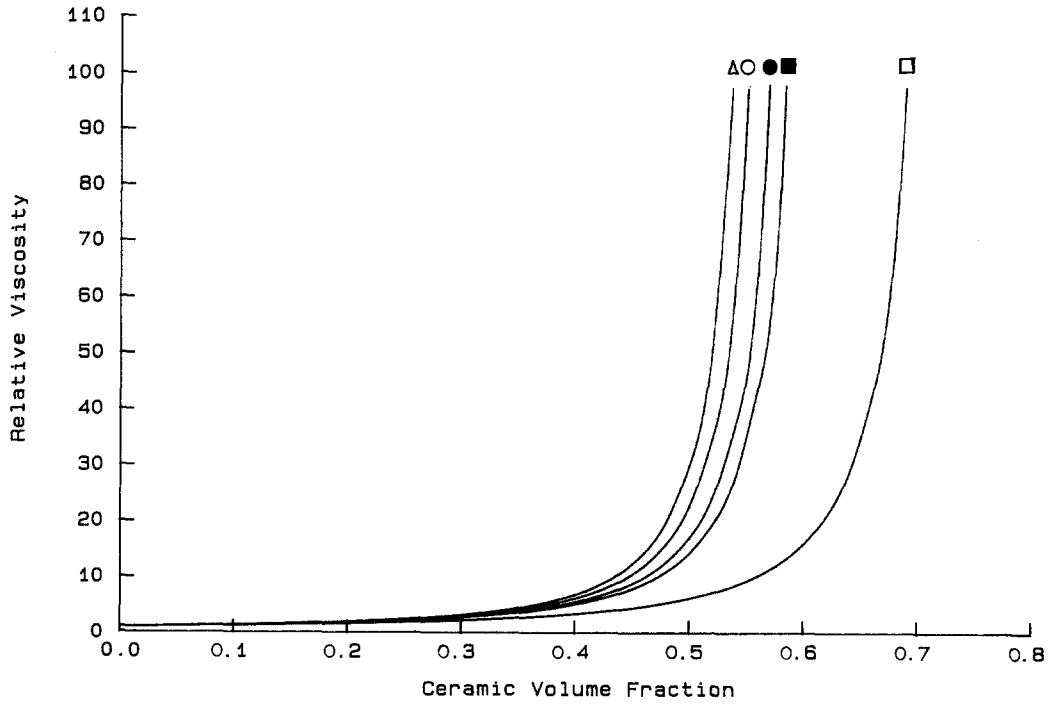

Figure 10 Viscosity–volume fraction curves for composites in the 0 to 30 vol % whisker content range based on Chong's equation: V_{max} = (□) 0.750, (■) 0.635, (●) 0.620, (○) 0.600 and (△) 0.584.

give

$$\eta_r = A + BW + CW^2 + DW^3 \quad (8)$$

in the region 0 to 30 vol % whisker additions where W is the volume fraction of whiskers based on the total ceramic volume and where η_r is the viscosity of a composite suspension divided by the viscosity of the binder. Thus for zero whisker loading the relative viscosity is 6.4. Although Equation 8 is an empirical relationship, it allows the prediction of viscosity over a range of whisker contents. The values of the coefficients in Equation 8 which yield a best fit to the experimental data are $A = 6.4$, $B = 10.5$, $C = -48.1$ and $D = 900.1$.

A considerably more powerful method of mapping the viscosity of these suspensions is again to employ Chong's equation and to use the contour map in Fig. 6 to predict V_{max} for the 50 vol % ceramic blends with different whisker loadings. Thus each point in Fig. 9 can be considered to lie on a separate Chong plot of the type shown in Fig. 5. Fig. 10 shows the family of Chong plots for these compositions and this method allows the prediction of viscosity for any composite in the useful composition range of 0 to 30% whisker addition.

It is also of interest to see how V_{max} varies with whisker content. In Fig. 11, V_{max} from Chong's equation is plotted against whisker content. This

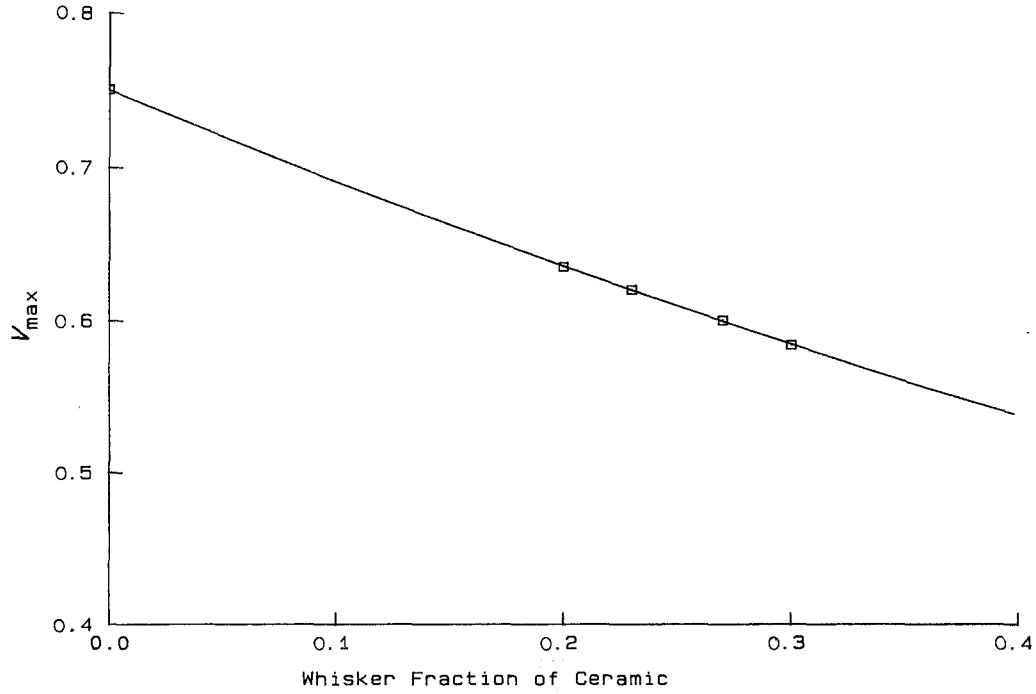

Figure 11 V_{max} from Chong's equation plotted against whisker content.

curve gives an indication of how the maximum packing efficiency of powder–rod systems varies with composition and can be compared with the results of Milewski's experiments [39]. From Milewski's results, using an aspect ratio of 16, a ratio (R) of particle diameter to fibre diameter of 1 and 25 vol % fibres (the nearest composition to that used in the present work), the maximum solids loading of 59.9 vol % is predicted. This compares reasonably with the V_{max} = 61 vol % found by Chong's equation for the composite system for a whisker fraction of 25 vol % from Fig. 11. The aspect ratio of whiskers which had been processed by this route was measured experimentally and gave an average value of 15 [20]. However, the agreement may be fortuitous in that the average aspect ratio conceals wide variations.

The curve fits an equation of the type

$$V_{max} = A + BW + CW^2 \quad (9)$$

where W is the whisker volume (%) based on the total ceramic volume and $A = 0.75$, $B = -0.616$, $C = 0.211$.

By substituting $W = 1$ into Equation 9, the curve (Fig. 11) is extrapolated to the situation where all the silicon nitride powder has been replaced by silicon carbide whiskers. Under these circumstances, V_{max} = 0.35. Thus the maximum isotropic packing fraction of the processed whiskers is predicted. Milewski [39] plotted accumulated packing fraction data for fibres as a function of aspect ratio. From his curve an aspect ratio of 15 is obtained for $V_{max} = 0.35$; a value which also agrees with experimentally determined aspect ratios for the silicon carbide whiskers after processing by twin screw extrusion [20]. Again this agreement is partly fortuitous in that the average whisker aspect ratio conceals wide variations and that whisker length degradation is enhanced at higher whisker contents.

4. Conclusions

Ceramic injection moulding compositions containing silicon nitride powder with and without silicon carbide whisker additions have been prepared. The relative viscosity, recorded at the ideal processing temperature and at the lower end of the shear rate range encountered in injection moulding were found to fit the equation of Chong *et al.* This was the case for powder and composite suspensions. This provided a method for the optimization of ceramic volume loading from a single viscosity measurement by a contour map derived from Chong's equation.

A similar procedure was used to investigate silicon nitride powder–silicon carbide whisker suspensions. In this way the viscosity of composite blends of powder and whiskers could be predicted over the volume loading range 0 to V_{max} and for whisker fractions from 0 to 0.3 based on the ceramic.

Acknowledgements

The authors thank SERC for support and the staff at T & N Technology Laboratories for their help.

References

1. E. A. BARRINGER and H. K. BOWEN, *Commun. Amer. Ceram. Soc.* **65** (1982) C199.
2. F. F. LANGE, *Phil. Mag.* **22** (1970) 983.
3. *Idem, J. Mater. Sci.* **17** (1982) 225.
4. G. C. WEI and P. F. BECHER, *Amer. Ceram. Soc. Bull.* **64** (1985) 298.
5. K. M. PREWO and J. J. BRENNAN, *J. Mater. Sci.* **15** (1980) 463.
6. J. HOMERY, W. L. VAUGHN and M. W. FERBER, *Amer. Ceram. Soc. Bull.* **67** (1987) 333.
7. S. C. SAMANTA and S. MUSIKANT, *Ceram. Engng Sci. Proc.* **6** (1985) 663.
8. P. D. SHALEK, J. J. PETROVIC, G. F. HURLEY and F. D. GAC, *Amer. Ceram. Soc. Bull.* **65** (1986) 351.
9. K. T. FABER and A. G. EVANS, *Acta. Metall.* **31** (1983) 565
10. S. J. BULJAN, J. G. BALDONI and M. L. HUCKABEC, *Amer. Ceram. Soc. Bull.* **66** (1987) 347.
11. R. LUNDBERG, L. WAHLMAN, R. POMPE and R. CARLSSON, *ibid.* **66** (1987) 330.
12. T. KANDORI, S. KOBAYASHI, S. WADA and O. KAMIGAITO, *J. Mater. Sci. Lett.* **6** (1987) 1356.
13. M. J. EDIRISINGHE and J. R. G. EVANS, *Int. J. High Tech. Ceram.* **2** (1986) 1.
14. *Idem, ibid.* **2** (1986) 249.
15. *Idem, J. Mater. Sci.* **22** (1987) 269.
16. H. L. FRISCH and R. SIMHA, in "Rheology: Theory and Applications". Edited by F. R. Eirich (Academic, New York, 1956) pp. 525–613.
17. J. V. MILEWSKI, *Ind. Eng. Chem. Prod. Res. Dev.* **17** (1978) 363.
18. J. K. WRIGHT, M. J. EDIRISINGHE, J. R. G. EVANS and J. ZHANG, to be published.
19. J. A. BRYDSON, "Flow Properties of Polymer Melts" (George Goodwin, London, 1981) pp. 21–25.
20. S. J. STEDMAN, J. R. G. EVANS and J. WOODTHORPE, *J. Mater. Sci.* **25**, 2A (1990) 1025.
21. F. P. BOWDEN and D. TABOR, "The Friction and Lubrication of Solids" (Clarendon, Oxford, 1950) pp. 185–7.
22. H. EILERS, *Kolloid Z.* **97** (1941) 313.
23. M. MOONEY, *J. Colloid. Sci.* **6** (1951) 162
24. J. S. CHONG, E. B. CHRISTIANSEN and A. D. BAER, *J. Appl. Polym. Sci.* **15** (1971) 2007.
25. J. W. GOODWIN, *Coll. Sci.* **2** (1975) 246.
26. R. J. FARRIS, *Trans. Soc. Rheol.* **12** (1968) 281.
27. N. OUCHIYAMA and T. TANAHRA, *Ind. Eng. Chem. Fundam.* **19** (1980) 338.
28. *Idem, ibid.* **20** (1981) 66.
29. *Idem, ibid.* **23** (1984) 490.
30. D. I. LEE, *J. Paint Technol.* **42** (1970) 579.
31. T. C. PUTTON, "Paint Flow and Pigment Dispersion" (Wiley, New York, 1979) p. 150.
32. R. K. GUPTA and S. G. SESHADRI, *J. Rheol.* **30** (1986) 503.
33. K. HUNT, J. R. G. EVANS and J. WOODTHORPE, *Br. Ceram. Trans. J.* **87** (1988) 17.
34. R. J. CROWSON, M. J. FOLKES and P. F. BRIGHT, *Polym. Engng. Sci.* **20** (1980) 925.
35. R. J. CROWSON and M. J. FOLKES, *ibid.* **20** (1980) 934.
36. J. G. BRODNYAN, *Trans. Soc. Rheol.* **III** (1959) 61.
37. T. KITANO, T. KATOAKA and T. SHIROTA, *Rheol. Acta.* **20** (1981) 207.
38. J. M. LUNT and J. B. SHORTFALL, *Plastics and Rubber Processing* September (1979) 108.
39. J. V. MILEWSKI, *Adv. Ceram. Mater.* **1** (1986) 36.

Received 16 January
and accepted 24 August 1989